

## An investigation into using benzohydroxamic acid as a collector for sulfide minerals

Shiva Mohammadi-Jam, Ziyi Li, Neil Rose, Kristian E. Waters

Department of Mining and Materials Engineering, McGill University, 3610 University Street, Montreal, Quebec H3A 0C5, Canada

Corresponding author: [kristian.waters@mcgill.ca](mailto:kristian.waters@mcgill.ca) (Kristian E. Waters)

**Abstract:** The mining industry aims to promote responsible chemical use during mineral processing operations to minimize the chemical contamination. Hydroxamic acids, which can form strong chelates with metals, have been shown to have less health and environmental issues when compared to xanthate collectors. In this work, the performance of benzohydroxamic acid (BHA) as a collector for galena, chalcopyrite, and quartz was evaluated. The minerals were conditioned with different concentrations (1.5, 3, and 4.5 kg/t) of collector at pHs 8, 9, and 10. The result showed that the treatment of the mineral surfaces with BHA enhanced the flotation recoveries of the sulfide minerals. High concentrations of benzohydroxamate anion, the protonic dissociation product of BHA, existed at basic pHs, where a chemical reaction between the anion and a metal cation on the mineral surface resulted in the adsorption of the collector onto the mineral surface. The microflotation results showed that the BHA collector was able to successfully recover galena and chalcopyrite. Their flotation recovery was dependent on the conditioning pH. Galena showed a high flotation recovery (up to 86%) at pH 9, whereas chalcopyrite became most hydrophobic at pH values of 8 and 9 (up to 88%). None of the BHA concentrations or conditioning pHs was able to enhance quartz recovery beyond 7%. The research results have implications in the application of BHA for the froth flotation of galena and chalcopyrite.

**Keywords:** galena, chalcopyrite, flotation, hydroxamate, benzohydroxamic acid

### 1. Introduction

In recent years, there has been an increasing focus on sustainable and responsible mining practices. Mining companies and mineral processors are becoming more aware of their environmental responsibilities and working towards minimizing their impact on the environment. Government regulations and public pressure also play a crucial role in driving the adoption of health- and environment-friendly mining plans. Xanthate collectors have been widely used as effective collectors in the flotation of sulfide minerals. However, they generate toxic compounds, such as carbon disulfide, upon decomposition. Therefore, despite being excellent collectors, efforts are made in modern mineral processing practices to mitigate their environmental impact. Hydroxamic acids, however, are chemically more stable and are generally considered to be less toxic, and offer some environmental advantages over xanthate compounds, making them attractive options for environmentally conscious operations (Elizondo-Álvarez et al., 2021). They have strong stability against hydrolyzation, oxidation, or decomposition (Yao et al., 2022).

Hydroxamic acids (RCONHOH) are organic compounds, known for their high chelating power with metal ions. The complexes formed between bidentate ligands of hydroxamic acids and their N-substituted derivatives and metal ions, such as Fe<sup>3+</sup> and Cu<sup>2+</sup>, are highly colored, and hence are used to analyze metal ions or hydroxamates by calorimetric techniques (Lipczynska-Kochany, 1991). Their ability of forming stable complexes with metal ions makes hydroxamic acids and their salts useful in various chemical applications, including the application as flotation collector for ore beneficiation. The use of hydroxamic acid collectors in froth flotation can offer several advantages, such as improved flotation performance and higher selectivity towards certain minerals, including rare earth (Meng et al.,

2015, Pavez and Peres, 1993, Pradip and Fuerstenau, 1983, Ren et al., 1997, Zhang et al., 2017) and non-sulfide (Bulatovic, 2010, Elizondo-Álvarez et al., 2020, Gibson et al., 2015, Lee et al., 1998, Lee et al., 2009, Li et al., 2020, Marion et al., 2017, Wang et al., 2016, Yao et al., 2018, Zhou et al., 2015), as well as sulfide (Elizondo-Álvarez et al., 2020) minerals.

Benzohydroxamic acid (BHA) with the chemical formula  $C_6H_5CONHOH$  is a chelating reagent with a bidentate group ( $HO-N-C=O$ ). BHA is known for its ability to form strong chelates with metal ions (Adiguzel et al., 2017, Kozlov et al., 2013, Schraml, 2000). It has been evaluated as collector in froth flotation of wolframite (Liu et al., 2019, Yang et al., 2014), monazite and dolomite (Espíritu et al., 2018), cassiterite (Cao et al., 2020, Tian et al., 2018, Tian et al., 2017, Tian et al., 2018), ilmenite (Fang et al., 2018, Xu et al., 2017), smithsonite (Wang et al., 2017), malachite (Zhang et al., 2021), rutile (Cao et al., 2019), muscovite mica (He et al., 2018), scheelite (Han et al., 2017, Wei et al., 2020), and rhodochrosite (Cui et al., 2023) minerals, as well as including pyrochlore-bearing (Gibson et al., 2017, Gibson et al., 2015) and rare earth (Jordens et al., 2016) ores. The adsorption mechanism of hydroxamic acids on the mineral surfaces, which involves a combination of chemical and physical interactions, can vary depending on the type of mineral and frother, pH, temperature, and presence of other chemicals, such as metal cations in the flotation system (Khalil and Fazary, 2004, Pavez and Peres, 1993, Tian et al., 2018). BHA, which is mainly at the keto state (Plapinger, 1959), has a polar functional group (hydroxamic acid) that consists of an oxygen and a nitrogen atom (Fig. a). The dissociation equilibrium constant,  $pK_a$ , of BHA ( $pK_{BHA}$ ) is between 8 and 9 (Elizondo-Álvarez et al., 2021, Liu et al., 2019, Tian et al., 2017, Xu et al., 2017), meaning that at lower pH values, it is predominantly in neutral form, as shown in Fig. 1a. At higher pHs, it is mainly in the form of benzohydroxamate anion (deprotonated form), which exists predominantly in two forms in approximately equal concentrations (Fig. 1b and 1c). A third form of anion was also suggested (Fig. 1d) however in very low concentrations, compared to the former two ( $10^{-4}$ - $10^{-3}$  times less) (Steinberg and Swidler, 1965). Which one of N-deprotonation or O-deprotonation will primarily take place upon acidic dissociation depends on the reaction condition (Supuran, 2013). The second deprotonation of hydroxamic acids is also possible, which only occurs in strongly basic solutions, producing hydroximate dianions (Adiguzel et al., 2017, Citarella et al., 2021). The three functional groups, shown in Fig. 1c-1d, can form coordination complexes with metal ions present on the mineral surface. The most typical reported coordination occurs through deprotonated hydroxyl and carbonyl oxygen atoms of the ligand, forming five-membered chelates (Adiguzel et al., 2017, Ozsváth et al., 2019).

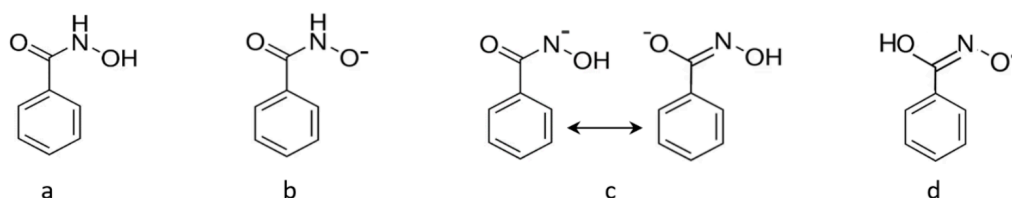


Fig. 1. Structure of a) benzohydroxamic acid in form of keto molecule and b, c, and d) hydroxamate anions in aqueous solutions

The strength of the interactions between the chelating ligands and metal ions depends on the metal cation. Potentiometric studies of the stability of the binary and ternary complexes of hydroxamic acids with metal cations indicated that the stability of the complexes depended on both chelator and metal cation, and follows the order salicylhydroxamic acid > benzohydroxamic acid > acetohydroxamic acid, and the ternary complexes of  $Fe^{3+} > Al^{3+} > Cr^{3+} > Cu^{2+} > Ni^{2+} > Co^{2+} > Zn^{2+}$  with some exceptions (Khairy et al., 1996, Khalil and Fazary, 2004); then rare earth metals (Pradip and Fuerstenau, 1983). Another study with salicylhydroxamic acid suggested the stability of the complexes in binary systems to be in the order  $Cu^{2+} \gg Co^{2+} > Ni^{2+} > Zn^{2+} > Cd^{3+} > Mn^{2+} > Mg^{2+} > Ca^{2+} > Ba^{2+} > Sr^{2+}$  (Khalil, 2000).

Although the application of various hydroxamate collectors in the froth flotation of a wide variety of minerals have been studied (Marion et al., 2017) and found to be effective reagents, the use of BHA in the flotation of galena and chalcopyrite is scarce in literature. This paper investigates the performance of benzohydroxamic acid (BHA) as collector in froth flotation of two sulfide minerals: galena and chalcopyrite, on a laboratory scale. The selectivity of the collector towards quartz, which usually coexist

as gangue with the two former minerals in sulfide ore deposits, was also studied. The compounds were characterized by elemental analysis and surface characterization.

## 2. Experimental

### 2.1. Materials

Galena (originating from Morocco), chalcopyrite (originating from Durango, Mexico), and quartz (originating from Godfrey, Ontario) were purchased from Ward's Science (USA). Potassium chloride (KCl), to be used as a background electrolyte, was obtained from Fisher Scientific (USA). Hydrochloric acid (HCl) and sodium hydroxide (NaOH) for pH adjustment, and methyl isobutyl carbinol (MIBC, C<sub>6</sub>H<sub>14</sub>O) frother were purchased from Sigma-Aldrich (Canada). Benzohydroxamic acid were purchased from Fisher Scientific (Canada).

### 2.2. Comminution and sizing

The galena and chalcopyrite samples were initially broken into approximately 2-3 cm pieces using a hammer and chisel. The two minerals along with quartz were then stage pulverized and screened using a Tyler Ro-Tap to separate +106  $\mu\text{m}$  from -106  $\mu\text{m}$  size fractions. Wet screening using a vibratory screen was conducted on the latter to produce -38  $\mu\text{m}$  and -106 +38  $\mu\text{m}$  size fractions. The latter were used for microflotation experiments. For zeta potential measurements, -38  $\mu\text{m}$  samples were further ground using a Planetary Mono Mill Pulverisette 6 (Fritsch, Germany) to produce -10  $\mu\text{m}$  samples.

### 2.3. Minerals characterization

X-ray diffraction (XRD) analysis was carried out on the mineral samples using a D8 Discovery X-Ray Diffractometer (Bruker, USA) equipped with a Co-tube as X-ray generating source ( $\lambda = 1.79 \text{ \AA}$ ). The resultant diffraction patterns were processed using Xpert High Score software (PANalytical) to identify peaks and relate them to the mineral samples. The specific surface areas of the mineral samples were determined by the N<sub>2</sub> Brunauer-Emmett-Teller (BET) technique, using a TriStar II Plus Surface Area and Porosity Analyzer (Micromeritics, USA). Particle size was determined using a Microtrac Series 5000 Sync Particle Size and Shape Analysis system (Microtrac, USA).

### 2.4. Zeta potential measurements

Electrophoretic zeta potential measurements were used to investigate the collector adsorption onto the mineral surfaces. The measurements were conducted using a NanoBrook ZetaPlus (Brookhaven Instruments, USA). 0.24 g of -10  $\mu\text{m}$  minerals was suspended in 10<sup>-3</sup> M KCl as background electrolyte. The KCl solution (containing BHA if applicable) was added until the final weight of the suspension reached 600 g (0.04 wt% solid). The suspension was then ultrasonicated for 45 s using a UP400S ultrasonic processor (Hielscher, Germany). The suspensions were conditioned for 30 min on a magnetic stirrer, which was kept on for the duration of the measurement in order to maintain particles suspended. The pH of the suspensions was adjusted using NaOH or HCl, and the suspensions were then allowed to equilibrate for 5 min before measurement. The pH range of the measurements was from 3 to 10 (the largest range possible with the equipment). The measurements were carried out in steps of 1 pH. To avoid zeta potential hysteresis, fresh suspensions were prepared for the acidic and basic zeta measurements.

### 2.5. Microflotation

The performance of BHA in the flotation of the minerals was evaluated by microflotation technique. The experiments were conducted with 1 g of -106 +38  $\mu\text{m}$  single mineral. The sample was conditioned for 5 min following the addition of 30 mL of the collector and pH adjustment. In the case of collectorless tests, the samples were treated with RO water. The conditioning and then flotation tests were conducted at pH 8, 9, and 10 with three different concentrations of BHA. The suspension was conditioned for one more minute after addition of a diluted solution of MIBC, which would produce a frother concentration of 15 ppm in 170-mL microflotation cell. After conditioning, the mineral suspension was transferred

into a Hallimond tube, and pH-adjusted RO water was added to bring the total volume of the cell to 170 mL. The flotation tests were conducted for 1 min using an air flow rate of 36 mL/min. A mini magnetic stir bar was used in the microflotation cell to keep the particles suspended throughout flotation. Upon completion, the concentrate and tailings were drained from the cell into their respective beakers. The contents of the beakers were then filtered, dried, and weighed to determine flotation recovery.

## 2.6. X-ray photoelectron spectroscopy (XPS)

X-ray photoelectron spectroscopy (XPS) measurements were conducted to study the chemical properties of the mineral surface and BHA adsorption. XPS was performed using Thermo Scientific K-alpha spectrometer (USA) with an Al K $\alpha$  X-ray source (1489.6 eV), applying a 400  $\mu$ m spot size, 50.0 eV pass energy, and 0.100 eV energy step size. In order to avoid charging on the surface, a flood gun was used to shoot the samples with low energy electrons during the experiments. The collected data was processed using Avantage Data Processing software (Thermo Fisher Scientific). The binding energy (BE) was calibrated using the background hydrocarbon C 1s binding energy of 284.8 eV.

## 2.7. Ultraviolet-Visible (UV-Vis) spectroscopy

The absorption spectroscopy experiments of BHA were performed using a Genesys 180 UV-Visible Spectrophotometer (ThermoFisher Scientific, USA). The analyses consisted of measuring the absorption of ultraviolet-visible light by different concentrations of the BHA collector at pH values from 3 to 10 over the wavelength range of 190-360 nm.

## 3. Results and discussion

### 3.1. Sample characteristics

The particle size analysis and BET specific surface area results are presented in Table 1. The samples of -106 +38  $\mu$ m size range were used for microflotation experiments and XPS analysis, and -10  $\mu$ m samples for zeta potential measurements and XRD analysis. Fig. 2 exhibits the X-ray diffraction patterns for the samples as well as the reference pattern for galena (Fig. 2a), chalcopyrite (Fig. 2b), and quartz (Fig. 2c) minerals. It demonstrates that all the characteristic peaks of the mineral samples correspond very well with the reference XRD patterns.

Table 1. Particle size, and specific surface area of the mineral samples

Mineral	Size range ( $\mu$ m)	D <sub>50</sub> ( $\mu$ m)	D <sub>80</sub> ( $\mu$ m)	BET specific surface area (m <sup>2</sup> /g)
Galena	-10	5.12	10.74	1.6024
	-106 +38	84.84	115.00	0.0865
Chalcopyrite	-10	3.46	9.45	5.8250
	-106 +38	81.27	106.80	0.2385
Quartz	-10	4.36	9.94	1.5879
	-106 +38	89.97	121.10	0.0916

### 3.2. Zeta potential measurements

The electrophoretic zeta potential results for galena, chalcopyrite, and quartz in the absence and presence of BHA are shown in Fig. 3a, 3b, and 3c, respectively. The data for galena displays a negative trend across the pH range investigated, and the magnitude of zeta potential increased at basic pH range, corresponding to previous work (Hu et al., 2021, Qin et al., 2015, Vergouw et al., 1998, Wang et al., 2018). However, the zeta potential trend for galena is slightly different in shape from the above-mentioned publications. Lower zeta potential values for pH 3, 4, and 5, in comparison to higher pH values, gives the curve a parabolic shape with a maximum value at pH 5 (Fig. 3a). A similar behavior was observed by (Subrahmanyam et al., 1990). It was suggested that at very low pH values, the adsorption of proton (H<sup>+</sup>)

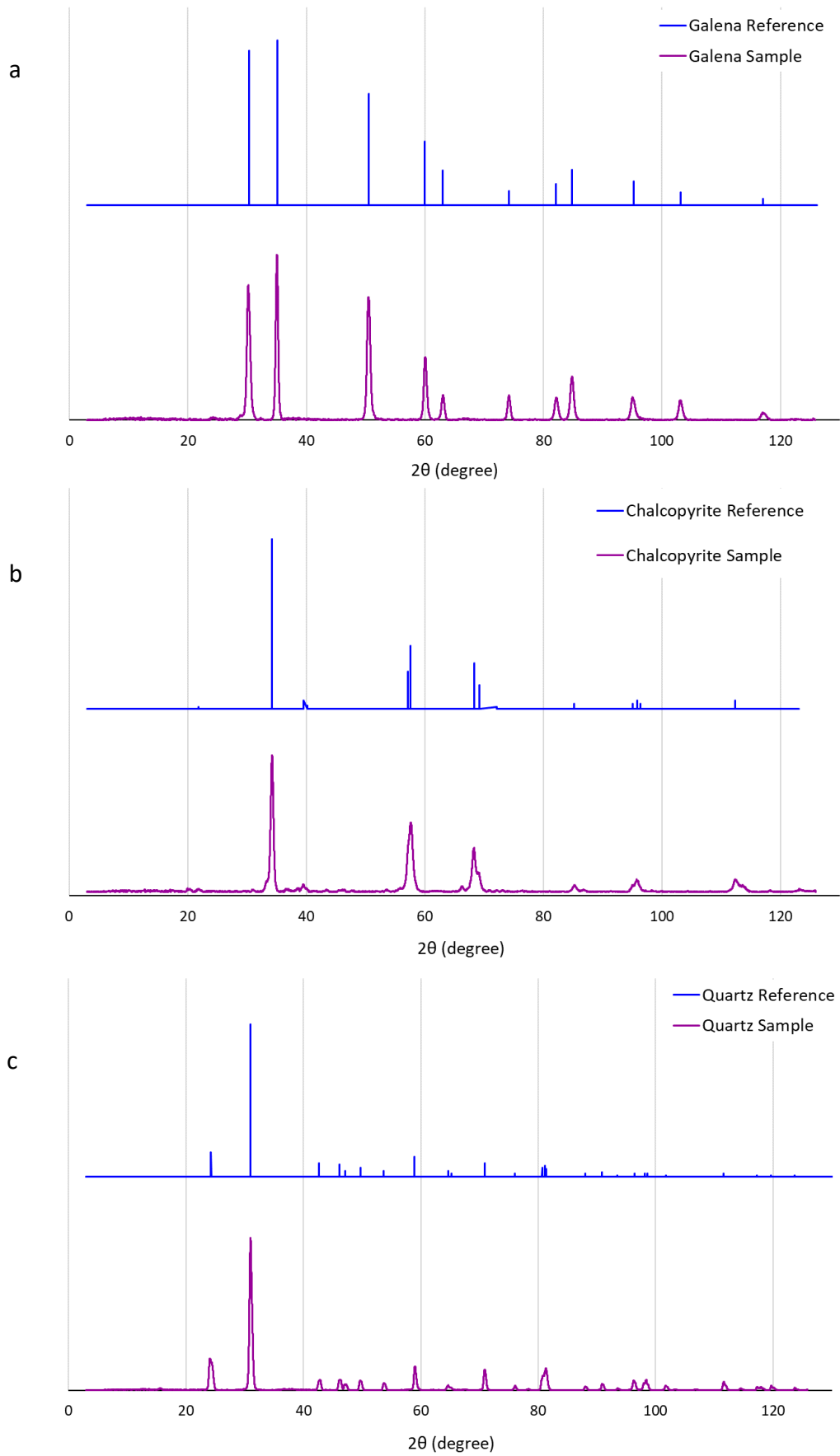


Fig. 2. XRD patterns of the mineral samples along with the reference patterns provided by the XRD processing software for galena (a), chalcopyrite (b), and quartz (c)

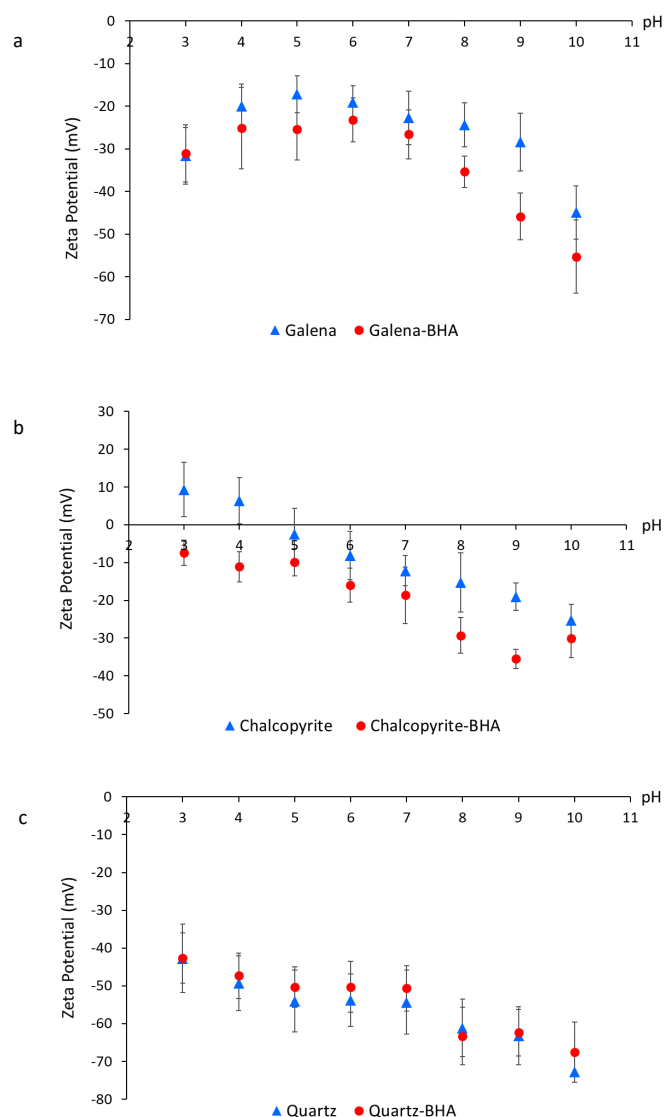


Fig. 3. Zeta potential trends of a) galena, b) chalcopyrite, and c) quartz in the presence and absence of BHA in 1 mM KCl solution. Error bars represent 95% confidence intervals

from the bulk solution onto the minerals surface is not quite stoichiometric. As a result, the surface becomes less negative (larger in magnitude) over the pH range of 2-4. Conditioning of galena surface with BHA resulted in more negative surface and the effect was more substantial at pH 8-10, indicating a stronger adsorption at this pH range. Since the surface of untreated galena was negatively charged over the whole pH range, it can be concluded that the adsorption of hydroxamate anion on the mineral surface occurs through chemical interaction rather than electrostatic attraction. At acidic pH, where BHA is mainly in molecular form, the concentration of the anion form to adsorb on the mineral surface is low. The acidic dissociation of the molecule around at pH > 8, produces benzohydroxamate anions which makes the galena surface even more negative upon coordinating with metal cations on the mineral surface.

The zeta potential results of chalcopyrite in the absence and presence of the collector are presented in Fig 3b. The zeta potential of untreated chalcopyrite decreased with increasing pH. The isoelectric point IEP of pristine chalcopyrite was 4.9, which corresponds very well to previous work (Liang et al., 2015). Conditioning with BHA had a significant effect on the zeta potential of chalcopyrite, and the surface became negatively charged throughout the investigated pH range and shifted the IEP to 2.2 (obtained through extrapolation). Here also the chemisorption of the benzohydroxamate anion onto the mineral surface resulted in a large difference in zeta potential before and after treatment at pHs 8 and 9.

As Fig. 3c demonstrates, the quartz surface was negatively charged across the examined pH range. The observed behavior was consistent with literature (Liu et al., 2018, Marion et al., 2017). Conditioning with BHA had little effect on the zeta potential values of quartz, suggesting little or no collector adsorption on the quartz surface.

It is noteworthy that wide discrepancies in zeta potential and IEP values, when comparing various studies on minerals, can be due to several factors, some of which can have a significant effect on the zeta potential values. These parameters include variation in sample preparation and experimental procedure, operation temperature, dissolved CO<sub>2</sub>, surface compositional differences due to the presence of impurities or oxidation, and mineral dissolution (Mohammadi-Jam et al., 2022).

### 3.3. Microflotation

The zeta potential results motivated the microflotation experiments of the single minerals to be conducted at pHs 8, 9, and 10 only. The flotation recoveries of galena, chalcopyrite, and quartz, conditioned with different concentrations of BHA at the three pH values are shown in Fig. 4a, 4b, and 4c, respectively, to evaluate the effect of the collector concentration and conditioning pH on the mineral flotation recovery. Flotation response is correlated with the presence of the precipitated metal-collector

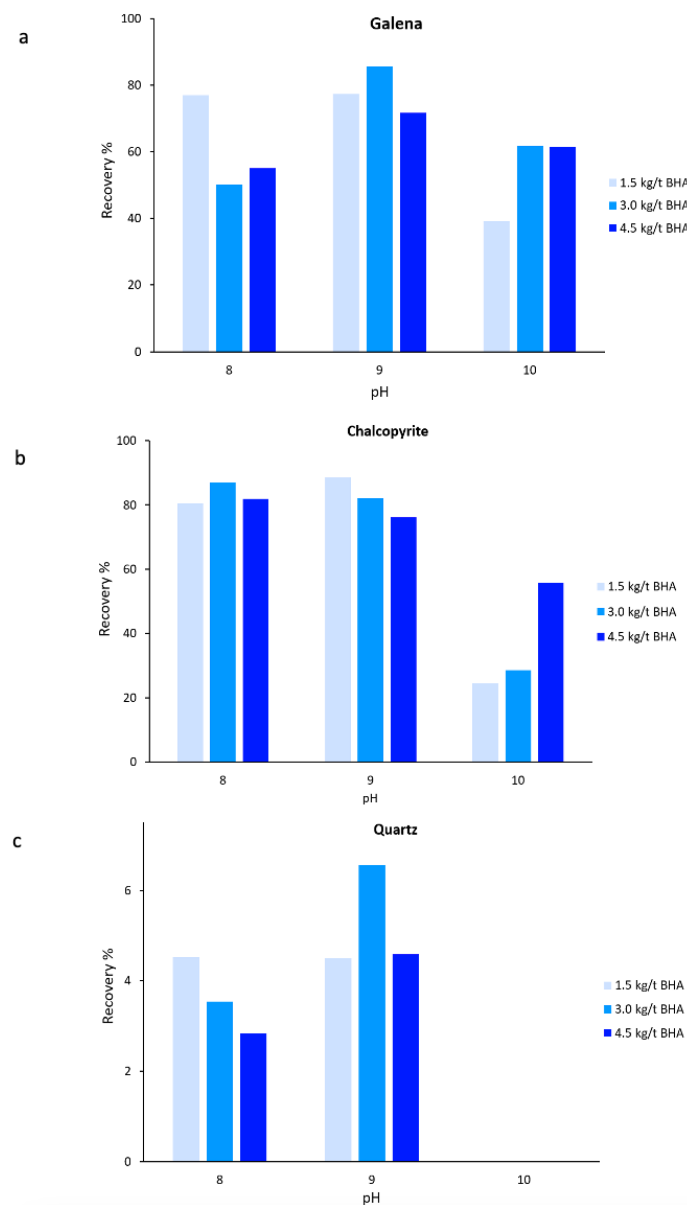


Fig. 4. Flotation recoveries of a) galena, b) chalcopyrite, and c) quartz, conditioned with three different concentrations of BHA at three pH values

species on the mineral surface. Considering the  $pK_{BHA}$  and zeta potential results, a good flotation performance was expected from BHA at pH values around 8-9. As shown in Fig. 4a and 4b, the both sulfide minerals showed high flotation recoveries of after their surfaces being conditioned with BHA collector. The microflotation results of galena, conditioned with 1.5 kg/t BHA solution at two pH 8 and pH 9 resulted in the same recovery (77%), while the floatability of the galena conditioned with the same BHA concentration showed a marked decline in strong alkaline condition (Fig. 4a). Applying a higher concentration of BHA (3.0 kg/t) at pH 9 seemed to provide a better condition for galena flotation, enhancing the flotation recovery up to 86%.

In the case of chalcopyrite, the performance of the three concentrations of BHA collector at both pH 8 and 9 was highest (up to 88% recovery) (Fig. 4b). The flotation recovery dropped at pH 10, which was more significant for the two lower concentrations. The behavior could be correlated with a high concentration of hydroxyl ions at pH 10, resulting in distribution of the adsorbed iron oxides and hydroxides, which are inherently hydrophilic, on the surface of chalcopyrite (Mielczarski et al., 1996, Wang et al., 2018). However, microflotation results show that the concentration of BHA does not have a consistent effect on the flotation of the minerals over the examined pH values.

Fig. 4c clearly shows that regardless of the collector concentration or pH, the flotation recovery of the common gangue mineral, quartz, does not improve significantly, if not at all, after conditioning with the BHA solution. These results were not unexpected as it was observed in the zeta potential results that the collector did not adsorb onto the quartz surface. The flotation recovery of quartz at pH 10 was zero for all three concentrations. This behavior should enable the separation of both galena and chalcopyrite from quartz.

### 3.4. XPS analysis

Fig. 5 shows the elemental compositions of the galena surface before and after conditioning with BHA. It demonstrates that nitrogen atom appeared on the galena surface after conditioning with BHA. Analyzing the high-resolution XPS spectrum of N 1s for the nitrogen detected on the galena surface after conditioning with BHA (Fig. 6a) led to two fitted peaks at 399.5 eV and 398.7 eV. In order to identify the components, the peak fitting of the N 1s spectrum of pure BHA was also conducted (Fig. 6b), giving two components with binding energies of 401.7 eV, attributed to N–C or N–(C=O)–O, and another peak at 399.6 eV, corresponding to N=C or N–O or N–(C=O) (Mohtasebi et al., 2016, Naumkin et al., 2012, Tardio et al., 2019). Both fitted peaks of N 1s shifted to lower binding energies after adsorption of BHA on the galena surface, possibly due to the interaction between nitrogen and metal and formation of new chemical bonds. Moreover, the difference between the background of N 1s of the galena surface and that of the pure BHA could be due to the inelastic scatter of electrons through the adventitious carbon layer on the natural mineral.

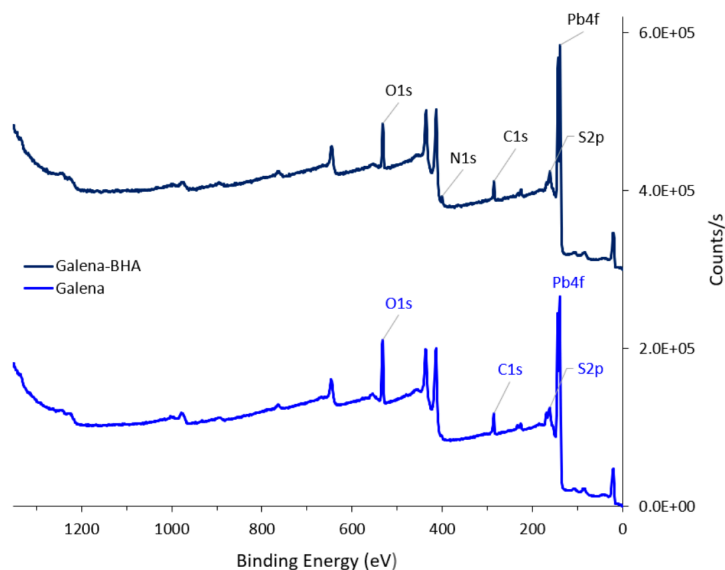


Fig. 5. XPS survey spectra of galena, before (bottom) and after (top) conditioning with BHA

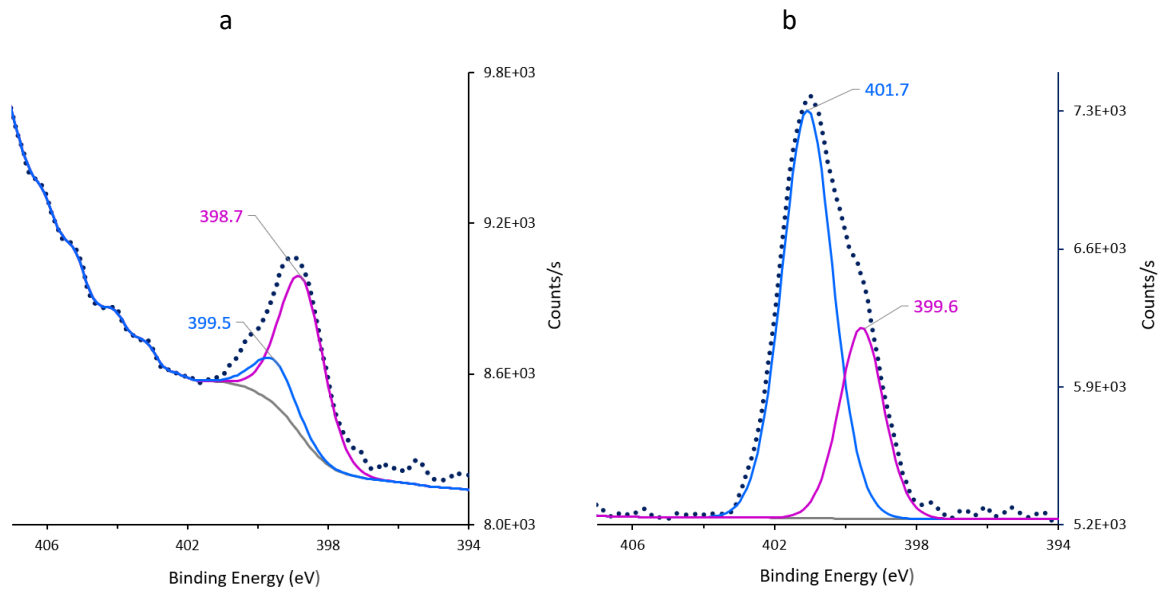


Fig. 6. High-resolution XPS spectra for N 1s of a) galena after conditioning with BHA, and b) pure BHA

Fig. 7 demonstrates the Pb 4f spectrum of galena before and after conditioning with BHA. The peaks located at 137.3 eV and 142.2 eV are galena characteristic peaks, while the other two at 138.9 eV and 143.7 eV represent the oxidation products of the lead ions on galena surface (Hu et al., 2021). The high intensity of the Pb-O peaks indicates that the galena surface was highly oxidized (Fig. 7a). After treating with BHA, the peak ratio of Pb-S to Pb-O decreased significantly (Fig. 7b), suggesting different behaviors of these two bonds upon conditioning the mineral with BHA. In addition, the binding energies of all peaks slightly increased after the treatment, which is an indication of the changes in the electronic density of the surface lead atoms due to the chemical coordination of Pb sites and BHA.

The survey spectra of chalcopyrite before and after conditioning with BHA are shown in Fig. 8a. Nitrogen atoms were present on the chalcopyrite surface before treatment; (Fig. 8a, top), however the concentration of nitrogen increased from 0.25 atomic% to 1.97 atomic%, which could be a result of the adsorption of the collector as the source of nitrogen. The quality of the high-resolution peak of N 1s in chalcopyrite was too low to accurately fit with the components. However, a peak value of 400.8 was reported by the Avantage software (Fig. 8b).

The high-resolution spectra of copper for chalcopyrite before and after surface treatment with the BHA collector are shown in Fig. 9. In the Cu 2p spectrum for untreated chalcopyrite, there are two chalcopyrite characteristic peaks from Cu<sup>+</sup> located at 931.9 eV and 951.8 eV. Two other peaks are also observed at 933.0 eV and 954.0 eV, which are attributed to the oxidized form of copper (Cu<sup>2+</sup>) on the

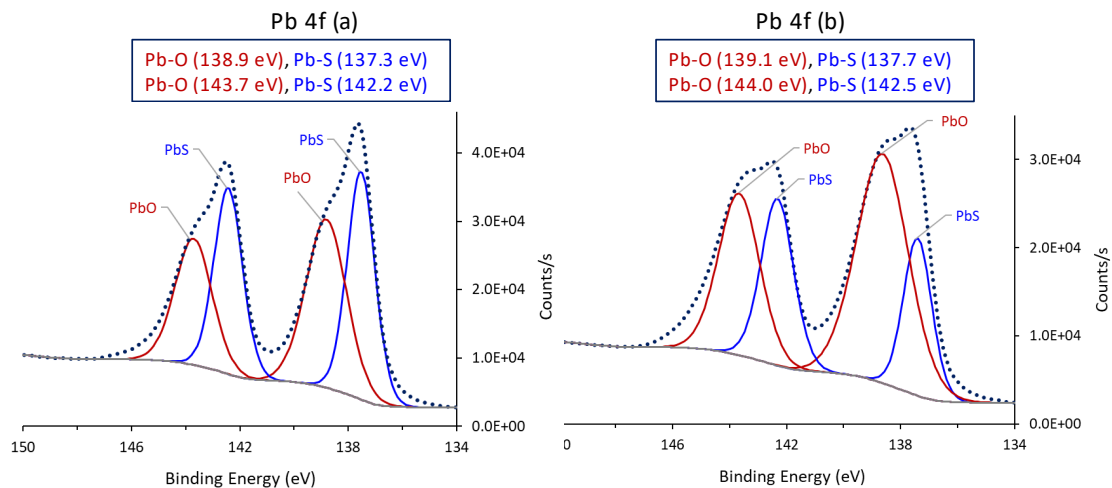


Fig. 7. High-resolution XPS spectra for Pb 4f of galena a) before and b) after conditioning with BHA

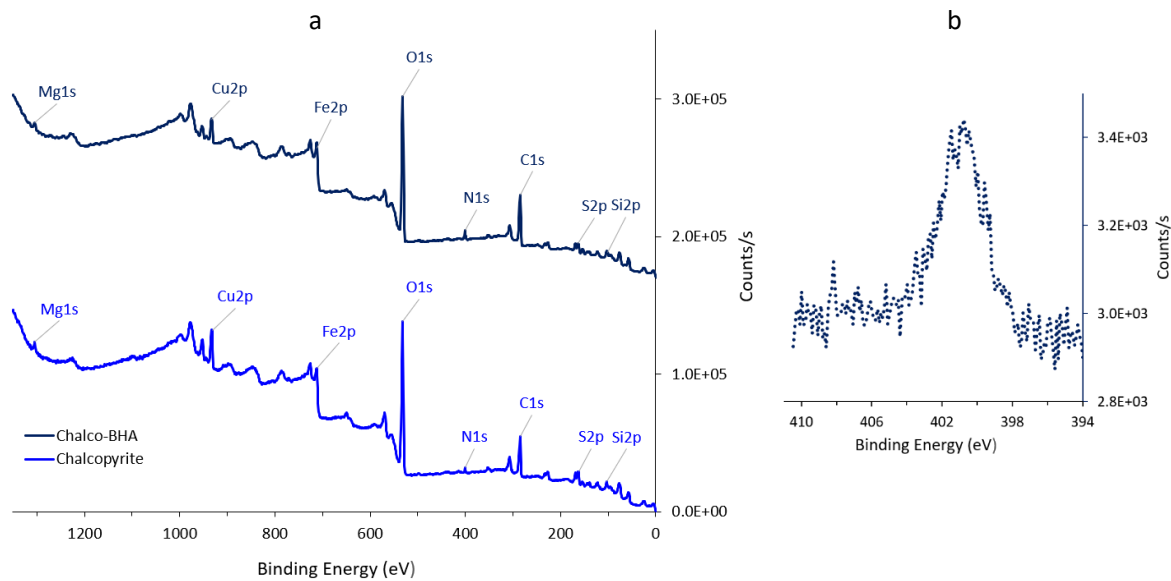


Fig. 8. a) XPS survey spectra of chalcopyrite before (bottom) and after (top) conditioning with BHA, and b) high-resolution XPS spectra for N 1s of the chalcopyrite surface after conditioning with BHA

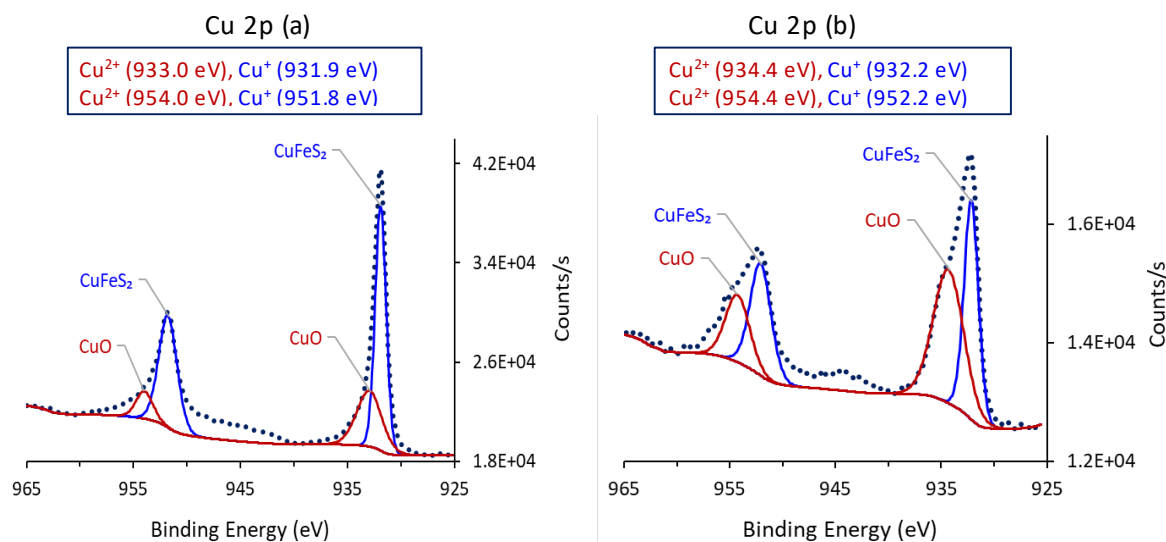


Fig. 9. High-resolution XPS spectra for Cu 2p of chalcopyrite a) before and b) after conditioning with BHA

surface of chalcopyrite (Fig. 9a). These results are consistent with the values previously reported in literature (Mielczarski et al., 1996, Zhang et al., 2022). After conditioning with the collector, the peak ratio of the first group ( $\text{Cu}^+$ ) to the second group ( $\text{Cu}^{2+}$ ) drastically decreased (Fig. 9b), which could be due to chemical adsorption of BHA on the chalcopyrite surface through coordination of benzohydroxamate anion with copper cation. Moreover, the binding energies of all four Cu 2p peaks shifted towards higher values upon surface conditioning with BHA, which is an indication of a decrease in electronic density around copper, probably because the metal cation acted as the coordination site with hydroxamate anion during the adsorption process. The evidence of BHA adsorption onto galena and chalcopyrite is consistent with the microflotation experiments.

### 3.5. UV-Vis spectroscopy

Fig. 10 shows the UV-Vis spectra of different BHA concentrations: 0.05, 0.10, and 0.15 g/L at pH values from 3 to 10, measured at the wavelength range of 190-360 nm. The concentrations of BHA were the same as the solutions used for the microflotation experiments. The spectra clearly indicate the effect of

pH on the dissociation behavior of BHA. Regardless of the acid concentration, a high intensity peak is observed at around 253 nm at pH values from 3 to 7. This peak, which corresponds to the protonated (neutral) form of the BHA acid, shows almost no changes with pH over this pH range, indicating the stability of the compound at acidic and neutral pH. At pH 8, a shoulder appeared at around 270 nm for 0.05 g/L BHA (Fig. 10a), which was more significant in the cases of 0.10 and 0.15 g/L (Fig. 10b and 10c, respectively). This signals the beginning of the protonic dissociation of the acid. When  $\text{pH} = \text{pK}_{\text{BHA}}$ , the concentrations of protonated BHA molecule and dissociated ion in the solution are equal. According to

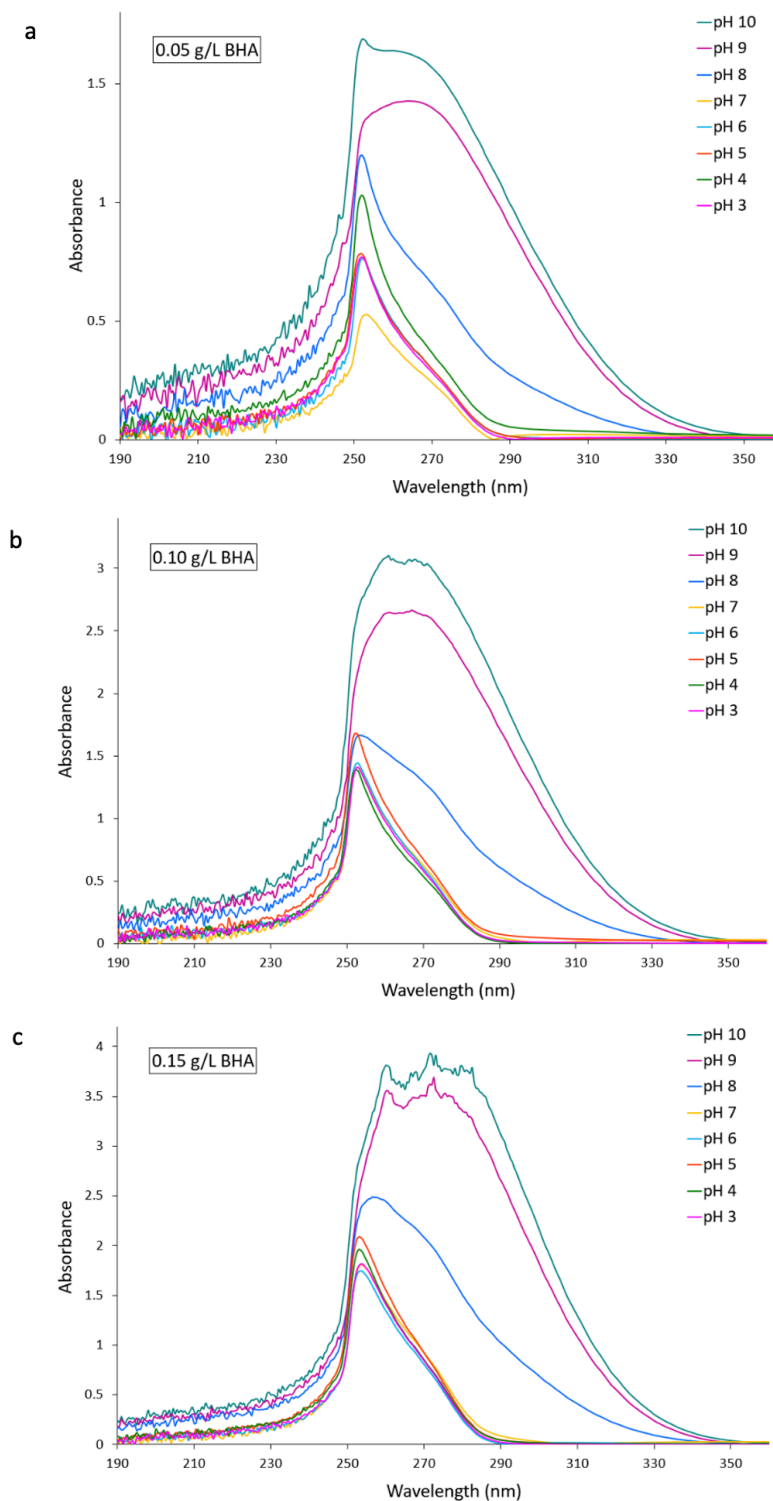


Fig. 10. UV-Vis absorption spectra for BHA solutions of three different concentrations: a) 0.05 g/L BHA, b) 0.10 g/L BHA, and c) 0.15 g/L BHA at pHs 3 to 10

UV-Vis spectra, this happens after pH 8. The anion concentration increases as pH increases, and in the UV-Vis spectra, a new broad peak appears at pHs 9 and 10 at higher wavelengths for all three concentrations. The appearance of the new peak with the highest absorbance between 260-272 nm is a clear indication of the presence of a different species in the solutions, which could be benzohydroxamate anion, produced from the first protonic dissociation of BHA. This wavelength range for benzohydroxamate anion is in good agreement with literature (Elizondo-Álvarez et al., 2021, Glorius et al., 2007, Plapinger, 1959). However, the authors found it difficult to find any publications reporting a close absorption wavelength for the molecular form of BHA. The reported wavelengths were 220 nm (Hassan et al., 2019), 224 nm (Hassan et al., 2018), and 227 nm (Elizondo-Álvarez et al., 2021, Fang et al., 2018, Glorius et al., 2007). It has been suggested however that the peak corresponded to the neutral form of BHA appears at 228 nm at low acidities, at 236 nm at intermediate acidities, and at high acidities at the region of 240-250 nm in sulfuric, hydrochloric and perchloric acid solutions (Ghosh, 2003). The latter is closer to the results presented here. The spiky signals observed in the case of 0.15 g/L BHA at pH 9 and pH 10 (Fig. 10c) could be due to the limits of the UV-Vis instrument. The progressive increase in the sample absorbance usually results in receiving very little light by the detector and generating fringe on the spectrum. Based on these results, at  $\text{pH} \leq 8$ , the molecular form of BHA is the dominant, and less active, species in the solutions. While at  $\text{pH} > 8$ , the acid molecule coexists with a higher concentration of benzohydroxamate anion, which can actively interact with metal cations. However, higher pH values will not necessarily lead to higher flotation recovery of minerals.

#### 4. Conclusions

The interactions of the benzohydroxamic acid (BHA) collector with three pure minerals: galena, chalcopyrite, and quartz were investigated. The research included the surface chemistry evaluation of the minerals and study the effects of BHA adsorption on the mineral flotation recovery. Microflotation experiments revealed that both sulfide minerals become highly hydrophobic after surface treatment with BHA solutions. While more work is required to determine the contribution of BHA concentration at different pH values for both sulfide minerals, it can be concluded that regardless of the collector concentration, galena showed a promising floatability after conditioning with the collector at pH 9. There is less difference in the case of chalcopyrite for the collector performance at pH 8 and 9; at which high recoveries were achieved. Quartz did not seem to change in terms of surface characteristics upon conditioning with BHA. XPS analysis demonstrated the changes in the peaks of coordinating metals. Significant changes in the peak ratios of different states of the lead and copper cations on the surfaces of galena and chalcopyrite, respectively, could be due to different tendency of the cations of different states towards benzohydroxamate anion. Further work is needed to determine how inevitable surface oxidation of sulfide minerals influences the flotation performance of BHA. The observed change in the UV-Vis spectra of BHA at various pHs was a clear indicator of the presence of different concentrations of benzohydroxamic acid molecule and benzohydroxamate anion, which could explain different behavior of the collector on the mineral surface at different pH values. According to the laboratory experiments, it can be suggested that benzohydroxamic acid could be considered a potential collector for the flotation of galena and chalcopyrite, and their separation from quartz.

#### Acknowledgments

The authors are grateful for the financial support from the Natural Sciences and Engineering Research Council of Canada (NSERC), Teck Resources Limited, COREM, SGS Canada Inc. and Flottec, under the Collaborative Research and Development Grants Program (grant number CRDPJ-531957-18).

#### References

- ADIGUZEL, E., YILMAZ, F., EMIRIK, M. OZIL, M., 2017. *Synthesis and characterization of two new hydroxamic acids derivatives and their metal complexes. An investigation on the keto/enol, E/Z and hydroxamate/hydroximate forms.* Journal of Molecular Structure 1127, 403-412.
- BULATOVIC, S. M., 2010. *Flotation of Oxide Copper and Copper Cobalt Ores.* Handbook of Flotation Reagents: Chemistry, Theory and Practice. S. M. Bulatovic. Amsterdam, Elsevier. 19, 47-65.

- CAO, M., GAO, Y., BU, H. QIU, X., 2019. *Study on the mechanism and application of rutile flotation with benzohydroxamic acid*. Minerals Engineering 134, 275-280.
- CAO, Y., SUN, L., GAO, Z., SUN, W. CAO, X., 2020. *Activation mechanism of zinc ions in cassiterite flotation with benzohydroxamic acid as a collector*. Minerals Engineering 156, 106523.
- CITARELLA, A., MOI, D., PINZI, L., BONANNI, D. RASTELLI, G., 2021. *Hydroxamic Acid Derivatives: From Synthetic Strategies to Medicinal Chemistry Applications*. ACS Omega 6(34), 21843-21849.
- CUI, K., JIN, S. DUAN, N., 2023. *Insights into the adsorption mechanism of benzohydroxamic acid in the flotation of rhodochrosite with Pb<sup>2+</sup> activation*. Powder Technology 427, 118705.
- ELIZONDO-ÁLVAREZ, M. A., URIBE-SALAS, A. BELLO-TEODORO, S., 2021. *Chemical stability of xanthates, dithiophosphinates and hydroxamic acids in aqueous solutions and their environmental implications*. Ecotoxicology and Environmental Safety 207, 111509.
- ELIZONDO-ÁLVAREZ, M. A., URIBE-SALAS, A. NAVA-ALONSO, F., 2020. *Flotation studies of galena (PbS), cerussite (PbCO<sub>3</sub>) and anglesite (PbSO<sub>4</sub>) with hydroxamic acids as collectors*. Minerals Engineering 155, 106456.
- ESPIRITU, E. R. L., DA SILVA, G. R., AZIZI, D., LARACHI, F. WATERS, K. E., 2018. *The effect of dissolved mineral species on bastnäsite, monazite and dolomite flotation using benzohydroxamate collector*. Colloids and Surfaces A: Physicochemical and Engineering Aspects 539, 319-334.
- FANG, S., XU, L., WU, H., TIAN, J., LU, Z., SUN, W. HU, Y., 2018. *Adsorption of Pb(II)/benzohydroxamic acid collector complexes for ilmenite flotation*. Minerals Engineering 126, 16-23.
- GHOSH, K. K., 2003. *Acid-base equilibria of hydroxamic acids: Spectroscopic investigation*. Indian Journal of Chemistry 42A, 2683-2697.
- GIBSON, C. E., HANSULD, R., KELEBEK, S. AGHAMIRIAN, M., 2017. *Behaviour of ilmenite as a gangue mineral in the benzohydroxamic flotation of a complex pyrochlore-bearing ore*. Minerals Engineering 109, 98-108.
- GIBSON, C. E., KELEBEK, S., AGHAMIRIAN, M. YU, B., 2015. *Flotation of pyrochlore from low grade carbonatite gravity tailings with benzohydroxamic acid*. Minerals Engineering 71, 97-104.
- GLORIUS, M., MOLL, H. BERNHARD, G., 2007. *Complexation of uranium(VI) with aromatic acids in aqueous solution – a comparison of hydroxamic acids and benzoic acid*. Radiochimica Acta 95(3), 151-157.
- HAN, H.-S., LIU, W.-L., HU, Y.-H., SUN, W. LI, X.-D., 2017. *A novel flotation scheme: selective flotation of tungsten minerals from calcium minerals using Pb–BHA complexes in Shizhuyuan*. Rare Metals 36(6), 533-540.
- HASSAN, L. R., BAHRON, H., RAMASAMY, K. TAJUDDIN, A. M., 2019. *Synthesis and AND Characterization of Benzohydroxamic Acid and Methylbenzohydroxamic Acid Meta Complexes and Their Cytotoxicity Study*. Malaysian Journal of Analytical Sciences 23(2), 263-273.
- HASSAN, L. R., RAMASAMY, K., LIM, S. M., BAHRON, H. MOHD TAJUDDIN, A., 2018. *Synthesis and Characterization of Benzohydroxamic Acid Metal Complexes and Their Cytotoxicity Study*. Jurnal Teknologi 80(6), 87-94.
- HE, J., HAN, H., ZHANG, C., XU, Z., YUAN, D., CHEN, P., SUN, W. HU, Y., 2018. *Novel insights into the surface microstructures of lead(II) benzohydroxamic on oxide mineral*. Applied Surface Science 458, 405-412.
- HU, Y., ZHAO, Z., LU, L., ZHU, H., XIONG, W., ZHU, Y., LUO, S., ZHANG, X. YANG, B., 2021. *Investigation on a Novel Galena Depressant in the Flotation Separation from Molybdenite*. Minerals 11(4), 410.
- JORDENS, A., MARION, C., GRAMMATIKOPOULOS, T., HART, B. WATERS, K. E., 2016. *Beneficiation of the Nechalacho rare earth deposit: Flotation response using benzohydroxamic acid*. Minerals Engineering 99, 158-169.
- KHAIRY, E. M., SHOUKRY, M. M., KHALIL, M. M. MOHAMED, M. M. A., 1996. *Metal complexes of salicylhydroxamic acid: Equilibrium studies and synthesis*. Transition Metal Chemistry 21(2), 176-180.
- KHALIL, M. M., 2000. *Complexation Equilibria and Determination of Stability Constants of Binary and Ternary Complexes with Ribonucleotides (AMP, ADP, and ATP) and Salicylhydroxamic Acid as Ligands*. Journal of Chemical & Engineering Data 45(1), 70-74.
- KHALIL, M. M. FAZARY, A. E., 2004. *Potentiometric Studies on Binary and Ternary Complexes of Di- and Trivalent Metal Ions Involving Some Hydroxamic Acids, Amino Acids, and Nucleic Acid Components*. Monatshefte für Chemie / Chemical Monthly 135(12), 1455-1474.
- KOZLOV, M. V., KLEYMENOVA, A. A., ROMANOVA, L. I., KONDUKTOROV, K. A., SMIRNOVA, O. A., PRASOLOV, V. S. KOCHETKOV, S. N., 2013. *Benzohydroxamic acids as potent and selective anti-HCV agents*. Bioorganic & Medicinal Chemistry Letters 23(21), 5936-5940.
- LEE, J. S., NAGARAJ, D. R. COE, J. E., 1998. *Practical aspects of oxide copper recovery with alkyl hydroxamates*. Minerals Engineering 11(10), 929-939.

- LEE, K., ARCHIBALD, D., MCLEAN, J. REUTER, M. A., 2009. *Flotation of mixed copper oxide and sulphide minerals with xanthate and hydroxamate collectors*. Minerals Engineering 22(4), 395-401.
- LI, Z., RAO, F., SONG, S., URIBE-SALAS, A. LOPEZ-VALDIVIESO, A., 2020. *Reexamining the adsorption of octyl hydroxamate on malachite surface: Forms of molecules and anions*. Mineral Processing and Extractive Metallurgy Review 41(3), 178-186.
- LIANG, Y.-T., ZHU, S., WANG, J., AI, C.-B. QIN, W.-Q., 2015. *Adsorption and leaching of chalcopyrite by Sulfolobus metallicus YN24 cultured in the distinct energy sources*. International Journal of Minerals, Metallurgy, and Materials 22(6), 549-552.
- LIPCZYNSKA-KOCHANY, E., 1991. *Photochemistry of hydroxamic acids and derivatives*. Chemical Reviews 91(4), 477-491.
- LIU, C., MIN, F., LIU, L., CHEN, J. DU, J., 2018. *Mechanism of hydrolyzable metal ions effect on the zeta potential of fine quartz particles*. Journal of Dispersion Science and Technology 39(2), 298-304.
- LIU, C., ZHANG, W., SONG, S. LI, H., 2019. *Study on the activation mechanism of lead ions in wolframite flotation using benzyl hydroxamic acid as the collector*. Minerals Engineering 141, 105859.
- MARION, C., JORDENS, A., LI, R., RUDOLPH, M. WATERS, K. E., 2017. *An evaluation of hydroxamate collectors for malachite flotation*. Separation and Purification Technology 183, 258-269.
- MENG, Q., FENG, Q., SHI, Q. OU, L., 2015. *Studies on interaction mechanism of fine wolframite with octyl hydroxamic acid*. Minerals Engineering 79, 133-138.
- MIELCZARSKI, J. A., CASES, J. M., ALNOT, M. EHRHARDT, J. J., 1996. *XPS Characterization of Chalcopyrite, Tetrahedrite, and Tennantite Surface Products after Different Conditioning. 1. Aqueous Solution at pH 10*. Langmuir 12(10), 2519-2530.
- MOHAMMADI-JAM, S., WATERS, K. E. GREENWOOD, R. W., 2022. *A review of zeta potential measurements using electroacoustics*. Advances in Colloid and Interface Science 309, 102778.
- MOHTASEBI, A., CHOWDHURY, T., HSU, L. H. H., BIESINGER, M. C. KRUSE, P., 2016. *Interfacial Charge Transfer between Phenyl-Capped Aniline Tetramer Films and Iron Oxide Surfaces*. The Journal of Physical Chemistry C 120(51), 29248-29263.
- NAUMKIN, A. V., KRAUT-VASS, A., GAARENSTROOM, S. W. POWELL, C. J. 2012. *NIST X-ray Photoelectron Spectroscopy Database, The Scienta ESCA300 Database Wiley Interscience*.
- OZSVÁTH, A., BÍRÓ, L., NAGY, E. M., BUGLYÓ, P., SANNA, D. FARKAS, E., 2019. *Trends and Exceptions in the Interaction of Hydroxamic Acid Derivatives of Common Di- and Tripeptides with Some 3d and 4d Metal Ions in Aqueous Solution*. Molecules 24(21), 3941.
- PAVEZ, O. PERES, A. E. C., 1993. *Effect of sodium metasilicate and sodium sulphide on the floatability of monazite-zirconite with oleate and hydroxamates*. Minerals Engineering 6(1), 69-78.
- PLAPINGER, R. E., 1959. *Ultraviolet absorption spectra of some hydroxamic acids and hydroxamic acid derivatives*. The Journal of Organic Chemistry 24(6), 802-804.
- PRADIP FUERSTENAU, D. W., 1983. *The adsorption of hydroxamate on semi-soluble minerals. Part I: Adsorption on barite, Calcite and Bastnaesite*. Colloids and Surfaces 8(2), 103-119.
- QIN, W., WANG, X., MA, L., JIAO, F., LIU, R., YANG, C. GAO, K., 2015. *Electrochemical characteristics and collectorless flotation behavior of galena: With and without the presence of pyrite*. Minerals Engineering 74, 99-104.
- REN, J., LU, S., SONG, S. NIU, J., 1997. *A new collector for rare earth mineral flotation*. Minerals Engineering 10(12), 1395-1404.
- SCHRAML, J., 2000. *Derivatives of hydroxamic acids*. Applied Organometallic Chemistry 14, 604-610.
- STEINBERG, G. M. SWIDLER, R., 1965. *The Benzohydroxamate Anion*. The Journal of Organic Chemistry 30(7), 2362-2365.
- SUBRAHMANYAM, T. V., SUN, Z., FORSSBERG, K. S. E. FORSLING, W., 1990. *Variables in the shear flocculation of galena. Sulphide deposits – their origin and processing*. P. M. J. Gray, G. J. Bowyer, J. F. Castle, D. J. Vaughan and N. A. Warner. Dordrecht, Netherlands, Springer, 223-231.
- SUPURAN, C. T., 2013. *Hydroxamates as Carbonic Anhydrase Inhibitors*. Hydroxamic Acids: A Unique Family of Chemicals with Multiple Biological Activities. S. P. Gupta. Berlin, Heidelberg, Springer Berlin Heidelberg, 55-69.
- TARDIO, S., ABEL, M.-L., CARR, R. H. WATTS, J. F., 2019. *The interfacial interaction between isocyanate and stainless steel*. International Journal of Adhesion and Adhesives 88, 1-10.

- TIAN, M., GAO, Z., SUN, W., HAN, H., SUN, L. HU, Y., 2018. *Activation role of lead ions in benzohydroxamic acid flotation of oxide minerals: New perspective and new practice*. Journal of Colloid and Interface Science 529, 150-160.
- TIAN, M., HU, Y., SUN, W. LIU, R., 2017. *Study on the mechanism and application of a novel collector-complexes in cassiterite flotation*. Colloids and Surfaces A: Physicochemical and Engineering Aspects 522, 635-641.
- Tian, M., Zhang, C., Han, H., Liu, R., Gao, Z., Chen, P., Wang, L., Li, Y., Ji, B., Hu, Y. Sun, W., 2018. *Effects of the preassembly of benzohydroxamic acid with Fe (III) ions on its adsorption on cassiterite surface*. Minerals Engineering 127, 32-41.
- VERGOUW, J. M., DIFEO, A., XU, Z. FINCH, J. A., 1998. *An agglomeration study of sulphide minerals using zeta-potential and settling rate. Part 1: Pyrite and galena*. Minerals Engineering 11(2), 159-169.
- WANG, D., JIAO, F., QIN, W. WANG, X., 2018. *Effect of surface oxidation on the flotation separation of chalcopyrite and galena using sodium humate as depressant*. Separation Science and Technology 53(6), 961-972.
- WANG, J., CHENG, H.-W., ZHAO, H.-B., QIN, W.-Q. QIU, G.-Z., 2016. *Flotation behavior and mechanism of rutile with nonyl hydroxamic acid*. Rare Metals 35(5), 419-424.
- WANG, Z., XU, L., WANG, J., WANG, L. XIAO, J., 2017. *A comparison study of adsorption of benzohydroxamic acid and amyl xanthate on smithsonite with dodecylamine as co-collector*. Applied Surface Science 426, 1141-1147.
- WEI, Z., HU, Y., HAN, H. SUN, W., 2020. *Configurations of lead(II)-benzohydroxamic acid complexes in colloid and interface: A new perspective*. Journal of Colloid and Interface Science 562, 342-351.
- XU, L., TIAN, J., WU, H., LU, Z., YANG, Y., SUN, W. HU, Y., 2017. *Effect of Pb<sup>2+</sup> ions on ilmenite flotation and adsorption of benzohydroxamic acid as a collector*. Applied Surface Science 425, 796-802.
- YANG, S., FENG, Q., QUI, X., GAO, Y. XIE, Z., 2014. *Relationship between flotation and Fe/Mn ratio of wolframite with benzohydroxamic acid and sodium oleate as collectors*. Physicochemical Problems of Mineral Processing 50(2), 747-758.
- YAO, W., LI, M., CUI, R., JIANG, X., JIANG, H., DENG, X., LI, Y. ZHOU, S., 2018. *Flotation Behavior and Mechanism of Anglesite with Salicyl Hydroxamic Acid as Collector*. The Journal of The Minerals, Metals & Materials Society (JOM) 70(12), 2813-2818.
- YAO, X., YU, X., ZENG, Y., MAO, L., XIE, H., LIU, S., HE, G., HUANG, Z., WANG, H. LIU, Z., 2022. *Behavior and Mechanism of a Novel Hydrophobic Collector in the Flotation of Bastnaesite*. Minerals 12(7), 817.
- ZHANG, C., ZHOU, Q., AN, B., YUE, T., CHEN, S., LIU, M., HE, J., ZHU, J., CHEN, D., HU, B. SUN, W., 2021. *Flotation Behavior and Synergistic Mechanism of Benzohydroxamic Acid and Sodium Butyl-Xanthate as Combined Collectors for Malachite Beneficiation*. Minerals 11(1), 59.
- ZHANG, J., ZHANG, X.-G., WEI, X.-X., CHENG, S.-Y., HU, X.-Q., LUO, Y.-C. XU, P.-F., 2022. *Selective depression of galena by sodium polyaspartate in chalcopyrite flotation*. Minerals Engineering 180, 107464.
- ZHANG, W., HONAKER, R. Q. GROPPPO, J. G., 2017. *Flotation of monazite in the presence of calcite part I: Calcium ion effects on the adsorption of hydroxamic acid*. Minerals Engineering 100, 40-48.
- ZHOU, F., YAN, C., WANG, H., SUN, Q., WANG, Q. ALSHAMERI, A., 2015. *Flotation behavior of four C18 hydroxamic acids as collectors of rhodochrosite*. Minerals Engineering 78, 15-20.